Research Article

Efficient Automatic Segmentation of Multi-Domain Imagery Using Ensemble Feature-Segmenter Pairs with Machine Learning

Prerna Pachunde[1], Dr.Sudhir.G.Akojwar[2]

R.C.E.RT, Chandrapur
prerna.dahiwade@gmail.com
G E C, Chandrapur
sudhirakojwar@gmail.com

Article History: Received: 11 January 2021; Revised: 12 February 2021; Accepted: 27 March 2021; Published online: 23 May 2021

Abstract: Automatic image segmentation refers to a field of study wherein images are analysed using complex colour, texture and shape-based features to decide the best possible segmentation configuration. These configurations differ in terms of algorithmic constants, image size, enhancement factors, edge thresholds, etc. To determine these constants, automatic segmentation algorithms use bio-inspired techniques like Genetic Algorithm (GA), particle swarm optimization (PSO), etc. These algorithms require re-training and re-evaluation whenever the input image type is changed. For instance, different set of edge thresholds are needed for medical resonance imagery (MRI) & natural images. Due to which a single algorithm is not applicable to solve the problem of multi-domain automatic image segmentation. To remove this drawback, this text proposes a novel ensemble-learning-based algorithm which uses feature-segmenter pairs for effective segmentation. The proposed approach is compared with existing state-of-the-art algorithms, and is found to have better peak-signal-to-noise ratio (PSNR) and moderate delay. The PSNR is improved by 10%, while keeping an optimum probabilistic random index (PRI) and delay performance.

Keywords: Automatic, image, segmentation, PSNR, PRI, ensemble

1. Introduction

Automatic or unsupervised image segmentation algorithms require lot of pre-processing and image analysis operations in order to segment the image [1]. These algorithms perform supervised segmentation to observe algorithmic constants, and then using the values of these constants performs unsupervised segmentation for new imagery. Such an approach can be observed in figure 1, wherein feature extraction, clustering, parameter evaluation, etc. can be observed. Approaches like these are found to be good for single domain images, wherein the application doesn't change much. But as the type of images is increased, this approach ceases to produce good results. This is due to the fact that image-type specific algorithmic constants have large variations. For instance, edge-based segmentation algorithms require edge thresholds to be tuned for effective segmentation, while color-based algorithms require effective red, green and blue thresholds for identification of segmentation regions. These thresholds remain almost constant for a single type of image, but as image type changes there are large variations in them.

If such systems are applied for multi-domain imagery then the output parametric performance reduces, and lower values of PSNR, PRI, etc. are obtained. In order to remove this drawback, this text proposes a novel ensemble-based feature-segmenter pair selection technique based on machine learning.

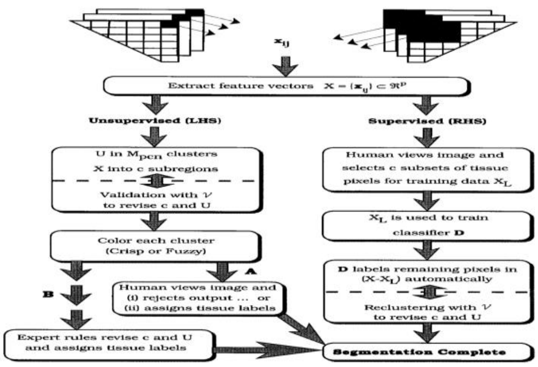

Figure 1. Example of an automatic image segmentation system.

Similar approaches are described by author's over-the-years. A review of these approaches can be observed in the next section, which is followed by the proposed approach and its parametric result evaluation. Finally, this text concludes with some interesting observations about the proposed approach, and suggests ways to improve the same.

2. Literature Review

Automatic image segmentation algorithms are generally focussed on segmenting images which belong to a particular domain. For instance, the work in [2] uses Regions with Convolutional Neural Networks or R-CNNs in order to segment out the Meniscus regions in Multispectral magnetic resonance imagery (MRIs). The algorithm is trained on more than 900 images, and produces an accuracy of more than 95%. This accuracy is an indicative of the segmentation performance for the given image domain. This high performance is achieved on MRI images, but the same algorithm can be trained for multiple datasets to obtain segmentation on different image types. Such a study can be taken up in order to evaluate the algorithm's performance for generalized images. An algorithm that uses fuzzy C means for generalized image segmentation is mentioned in [3]. In this algorithm Intuitionistic Fuzzy C-Means clustering algorithm is used along with Robust Statistics for efficient colour segmentation. PRI values in the range of 0.883 are obtained using this algorithm on different datasets. But the algorithm doesn't perform well on medical imaging. For that purpose, the deep neural network mentioned in [4] can be used. It performs unsupervised brain MRI segmentation with more than 84% accuracy when tested on Fluid-attenuated inversion recovery (FLAIR) brain tumor segmentation (BraTS) dataset. The algorithm uses a U-network which is based on DeepSeg architecture for effective image segmentation. Another such network can be observed in [5], wherein Multi-Modal MRI Brain Tumour Sub-Regions are segmented using a combination of contracting-bottleneck-expanding networks. The system is able to obtain a high PRI of 0.937 with the help of this network. But is applicable only for brain MRI imagery. A similar architecture for segmentation of Anterior Cruciate Ligament (present in knee MRIs) can be observed in [6]. This architecture also uses a similar network like [5], but adds depth information to it. The network is able to product PRI values in the range of 0.9 to 0.95, and is applicable for MRI data only. The performance of this network can be further enhanced using better CNN architectures like the ones mentioned in [7]. From the research in [7] it can be observed that VGGNet-based CNNs are better than AlexNet, while GoogLeNet and VGGNet have similar segmentation performance.

Automatic image segmentation can also be applied to lung computerized tomography (CT) imagery. The work in [8] proposes the use of super-pixel segmentation along with Trachea elimination and contour detection in order to improve the accuracy of segmentation. Due to this, the overall PRI values are improved to over 0.91, which can be further optimized with the help of CNN architectures. Moreover, the application of this system can be further expanded with the help of automatic fuzzy clustering framework (AFCF) as mentioned in [9]. The framework is able to segment multi-domain imagery with the help of similarity matrix and decision graphs. These graphs assist in finding out region confidence during image segmentation to obtain PRI values in the range of 0.95 to 0.98, which enables the application of this algorithm to real-time segmentation systems. The work in [7], [8] and [9] is combined in [10] to create a CNN that can perform unsupervised segmentation on multi-domain imagery. The work uses feature clustering using FCM and uses these clusters to obtain final segmentation with the help of an optimized CNN architecture. The architecture can be observed from figure 2, wherein an initial CNN is used for feature extraction. These features are clustered using FCM, and a back-propagation based CNN is used for final segmentation. Due to this complex process, the PRI values are in range of 0.97 to 0.99, which makes the system highly applicable to real-time multi-domain image segmentation.

Automatic image segmentation using G-mutual information is applied to plant leaf segmentation in [11]. The work uses mutual information combined with background estimation for leaf segmentation. This work produces an accuracy of more than 90% and a PRI of more than 0.93 when tested on multiple kind of leaf images. A similar architecture that uses mutual mean teaching can be observed in [12]. In this architecture multiple segmentation algorithms are combined with CNN using cross-entropy loss-reduction to improve segmentation performance. As a result of this a PRI of more than 0.89 is obtained on multi-domain images. Another CNN inspired model for unsupervised image segmentation can be observed in [13], wherein feature transformation subnetworks are combined with trainable deep clustering subnetwork (DCS) for better understanding of image structure. This results in a moderate PRI value of 0.84, which can be further improved using the CNN architecture mentioned in [10].

Skin images can also be segmented with the help of automatic segmentation. The work in [14] uses stack ensemble of deep and conventional image segmentation method for automatic segmentation of skin imagery. This method performs localization of vitiligo lesions in these images via a combination of different fast CNN architectures. Due to this combination an accuracy of more than 95%, and a PRI of more than 0.98 is obtained. This concept can be further expanded to retinal images. The work in [15,16] uses a similar learning model based on Markov random field (MRF) for identification of intensity and contextual information.

The work produces moderate PRI values in the range of 0.84, but can use CNNs to improve this value. Brain MRIs can also be segmented automatically with the help of self-organizing maps (SOMs) as mentioned in [17]. The work combines modified fuzzy K-means (MFKM) clustering with SOM for effective segmentation of brain tissues. This work produces an accuracy of 98%, and a high PRI value of 0.94 for MRI segmentation, and can be extended to other applications as well. Moreover, the clustering performance of MKFM can be improved using super-pixel clustering and morphological image processing as mentioned in [18, 19]. Learning from brain MRI can be transferred to CT imagery with the help of transfer learning architectures. Once such architecture is mentioned in [20], which uses unsupervised object discovery along with a CNN classifier for better segmentation results.

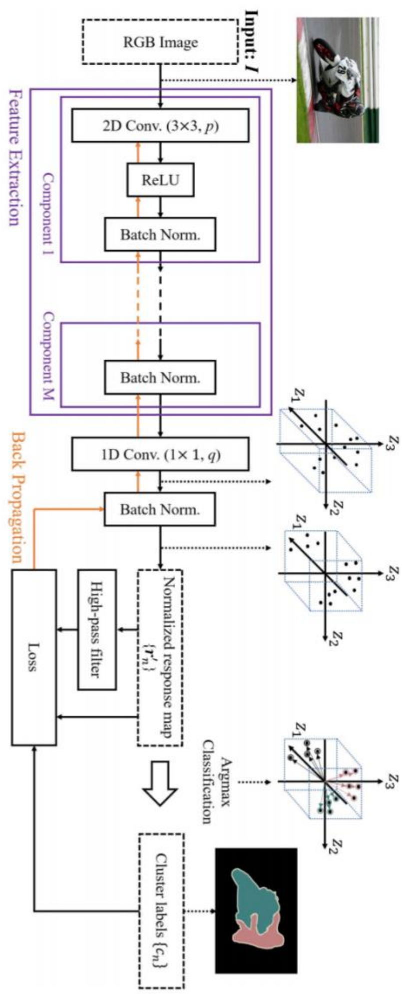

Figure 2. Integrated clustering with CNN for efficient segmentation [10]

Once such architecture is mentioned in [20], which uses unsupervised object discovery along with a CNN classifier for better segmentation results. The system uses a combination of LowRes CNN, fast convolutional network and U-network to achieve segmentation accuracies in the range of 97% to 99%, with a PRI between 0.98 to 0.99. A similar performing CNN that uses Mumford-Shah loss function can be observed in [21]. This CNN improves the performance obtained in [20], by making it applicable to multiple kinds of images, and using a semi-supervised training system.

Researchers in [22] have also considered the use of small-variance-asymptotic (SVA) combined with Bayesian estimator for performing multi-domain segmentation. As a result of combining SVA with Bayesian estimator the PRI values are in the range of 0.88 to 0.95, which can be improved by replacing SVA with CNN based architectures. Such an architecture can be observed from [23], which uses Generative Adversarial Networks (GANs) for improved classification performance. The network is used for segmenting Kidney imagery, but can be used for any kind of application with proper training. The GAN system is able to achieve an accuracy between 93% to 99% depending upon the input image set. Such networks can also be used for optical microscopic images [24] and multi-modal MR images [25] for better segmentation performance. X-Ray image segmentation is performed with the help of FCM in [26]. But the algorithm has low PRI and accuracy values, which can be improved with the help of GAN or CNN architectures as mentioned in [22-25]. Neural networks can CNNs can also be used for literature painting segmentation [27], Biobank cardiovascular magnetic resonance imaging studies [28], G-band chromosome image segmentation [29] and CT-image segmentation [30] as well. Thus, these networks have huge applicability. But they require large training delays which limits their application areas, therefore the proposed work mentioned in the next section; uses SVM-based classification in order to improve the performance of automatic image segmentation while keeping lower delay performance than its CNN counterparts.

3. Proposed machine learning approach for multi-domain image segmentation using ensemble feature-segmenter pairs

The proposed machine learning model uses multi-class support vector machines (mSVM) in combination with an ensemble of image segmentation algorithms to achieve the task of automatic image segmentation. Flow of the proposed architecture can be observed from figure 3, wherein a set of 10 different segmentation algorithms are used. The reason for selecting each of these segmentation algorithms is mentioned in table 1, which indicates the strength and applications for each of the algorithms.

Table 1. Reasons for selecting different segmentation algorithms for Ensemble.

Algorithm Name	Purpose of use
Canny-edge segmentation	Has good performance for Medical Resonance Imagery (MRI)
Prewitt-edge segmentation	Performs better for skeleton images and MRIs
Edge maximization (EM)	Optimally extracts edges which is useful for lung-image segmentation
Region growing (SRG)	Extraction of suggested region pixels based on colour levels is possible. This is used for colour-based segmentation in natural scenes and single object imagery.
Watershed algorithm	Applied to images where there are different areas or regions that need separate segmentation.
KMeans segmentation	Cluster-based segmentation, which combines pixels of similar colour together, thereby improving the overall segmentation performance. Applied to mammographic images, microscopic images, etc.
Fuzzy C Means (FCM) segmentation	Highly optimized clustering algorithm, which can be applied to natural scenes, medical imagery, single and multi-object segmentation images, etc.
KCM segmentation	It’s a hybrid of FCM and KMeans, and is used to optimally identify similar regions from multi-domain imagery.
Saliency map segmentation (SalM)	Its based on the quaternion domain of segmentation, and is used for optimally segmenting out regions of images where single objects are present. It uses a combination of colour and edge-based segmentation for high PSNR values.
Gray level co-occurrence integrated algorithm (GLCIA)	One of the most widely used texture segmentation algorithm. It is used for high quality texture analysis, which assists in multi-region segmentation.

With the help of ground truth image, minimum mean squared error (MMSE), peak signal to noise ratio (PSNR), delay, probabilistic random index (PRI) is evaluated for each of the algorithms. These parameters are evaluated using the following equations,

$$MMSE = \frac{\sum I_{seg} - I_{GT}}{N * M} \dots (1)$$

$$PSNR = 20 * \log_{10}\left(\frac{255}{MMSE}\right) \dots (2)$$

$$Delay = C_t - S_t \dots (3)$$

$$PRI = \left(\frac{1}{N * M}\right) * \sum I_{seg} * I_{GT} + \left(1 - I_{seg}\right) * (1 - I_{GT}) \dots (4)$$

Where, N is the number of columns, M is the number of rows, I_{seg} is the segmented image pixels, I_{GT} are the ground truth image pixels, C_t is the completion time, and S_t is the start time. Algorithms which have minimum delay value, maximum PRI and maximum PSNR value are selected as best segmentation algorithms for a given image. This information is stored as tags in the database, along with image features. In order to describe the image completely, the following image features are extracted,

3.1 Colour descriptor

This descriptor is used to describe colour variations in the input image. The following process is followed in order to evaluate this descriptor,

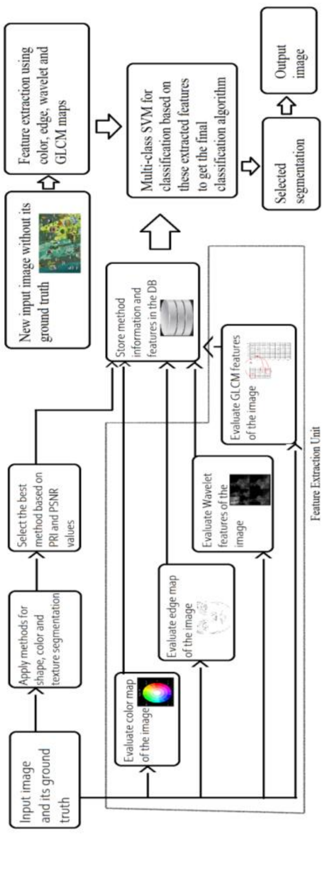

Figure 3. Architectural flow of the proposed system

1. The RGB image is converted into a 128-bit HMMD colour space.

2. A 128 bin HMMD quantization table (hue, diff, sum) is generated using. This uses Hue, Value and Saturation values

3. Image is converted from RGB 2 Indexed domain

4. This converted indexed image and the HMMD map are given to a pixel counting block to obtain the value of each pixel present in the indexed image viathe HMMD map.

5. This creates is a complex relation between the original RGB image pixel and the output count. This output count when plotted against the quantized pixel intensity is termed as image colour descriptor

3.2 Edge descriptor

Edge descriptor is responsible for evaluating the probability of edges for a particular pixel pair. The following process is followed to evaluate the edge map.

1. Get masks for horizontal, vertical, diagonal and anti-diagonal filtering to get the edge information

2. Filter the image using these masks

3. Determine the max edge of the averages in a 2x2 area

4. Create the main edge histogram to return.

5. Add vertical, horizontal and neighbouring groups to get the final edge map

This edge map conveys edge changes in the image, and thus is responsible for representing the image edges. This map is also termed as shape-map, as it determines shape changes in the image.

3.3 Wavelet descriptor

In order to determine the energy of pixels, a haar-wavelet descriptor is used. The following simplistic process is followed to obtain this descriptor,

1. Take input image, and keep applying haar wavelet transform till the image size becomes 8x8

2. Plot all pixels on Y axis and pixel number on X axis for all RGB values to obtain wavelet descriptor

3.4 Grey level co-occurrence matrix (GLCM) map

This matrix is responsible for showcasing relationships between the pixel-neighbours. For any image, the GLCM is sized as an 8x8 matrix. Combining all the RGB GLCM values results into a GLCM map, which is then used to determine mutual dependence of pixels on each other?

All these maps are combined together, and stored into a single array. This array is stored in database along with the selected segmentation algorithm. In order to train the multi-class SVM classifier, the selected segmentation algorithm is given as classes, and the feature vector is given as features to SVM. As each of the features has a different scale, thus 4 different SVM classifiers are trained. Outputs from each of these classifiers are used for selecting the final segmentation algorithm. The process of final segmentation selection can be observed from figure 4, wherein mode operation is performed in order to select the best possible segmentation algorithm.

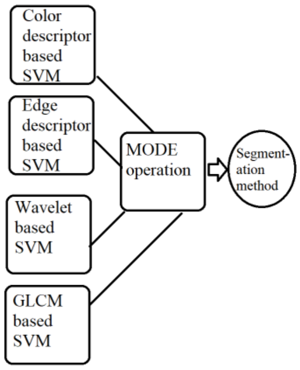

Figure 4. Mode operation for SVM output selection

Finally, the selected algorithm is used for image segmentation. MMSE, PSNR, Delay and PRI values are evaluated for the selected algorithm. These values are compared with existing state-of-the-art methods, and their performance comparison is done. This comparison can be observed from the next section, which indicates that the proposed algorithm has better performance than the compared methods.

4. Statistical Analysis

In order to perform statistical analysis of the proposed algorithm, following datasets were used,

- Weizmann database with single object consisting of 100 image samples
- Berkeley segmentation dataset consisting of 300 image samples

These datasets are combined and total 400 images are used for algorithmic evaluation. These datasets consist of multiple image types, and thus they are used for evaluation of the proposed algorithm. These images are divided into a ratio of 70:30 for training and testing. Thus, 280 randomly selected images are used for training, while the remaining 120 images are used for testing. Ground truth data of these image is already available with the dataset, thus MMSE, PSNR and PRI have been evaluated. The following table 2 showcases average PSNR values for different number of images (NI) on different algorithms.

Table 3. Average PSNR v/s number of images for each algorithm

NI	**SRG**	**KCM**	**SalM**	**GLCM**	**Proposed**
10	27.2	27.1	28.2	26.5	28.5
20	27.5	27.2	27.9	28.1	28.7
30	30.3	28.3	28.3	29.3	31.3
40	28.3	30.3	28.3	28.3	31.1
50	29.3	30.3	28.3	27.3	31.5
60	30.6	30.6	29.1	29.3	31.8

70	30.3	30.1	29.3	28.3	30.4
80	28.1	27.3	28.3	28.3	28.7
90	28.3	30.2	28.3	30.1	30.7
100	30.3	28.3	28.3	28.3	30.5
110	28.3	30.3	29.3	29.3	30.4
120	27.3	29.3	30.3	27.3	31.0

Similar analysis is done for PRI values, and the following results shown in table 3 are obtained,

Table 4. Average PRI v/s number of images for each algorithm

NI	**SRG**	**KCM**	**SalM**	**GLCM**	**Proposed**
10	0.860	0.840	0.814	0.917	0.860
20	0.891	0.836	0.819	0.933	0.891
30	0.853	0.924	0.897	0.958	0.953
40	0.925	0.895	0.899	0.950	0.971
50	0.854	0.901	0.973	0.929	0.962
60	0.901	0.899	0.925	0.931	0.963
70	0.899	0.875	0.948	0.862	0.953
80	0.941	0.888	0.888	0.899	0.963
90	0.908	0.878	0.977	0.956	0.976
100	0.977	0.861	0.861	0.903	0.967
110	0.869	0.872	0.952	0.955	0.960
120	0.907	0.897	0.899	0.936	0.964

Based on this analysis it can be observed from figure 5, that the proposed algorithm has better average PSNR values when compared with the existing algorithms. Similar trend can be observed for PRI values from figure 6, wherein a 10% improvement in PSNR and PRI can be observed.

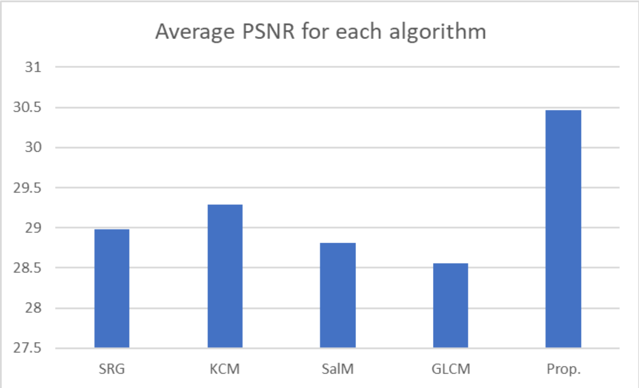

Figure 5. Average PSNR for each algorithm

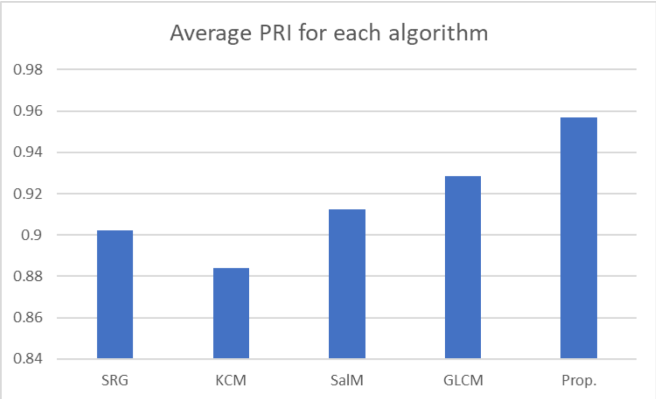

Figure 6. Average PRI for each algorithm

From this analysis it can be observed that the underlying algorithm can be applied for real-time automatic image segmentation purposes. Visual results for this segmentation can be observed from figure 7 (a) and 7 (b), where input images and their segmented outputs are seen. These images are extracted from Weizmann and Berkeley datasets respectively.

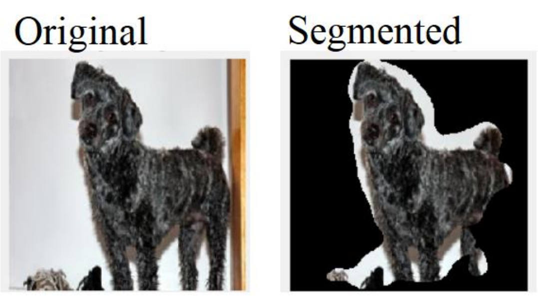

Figure 7. (a). Segmentation results for the Weizmann dataset

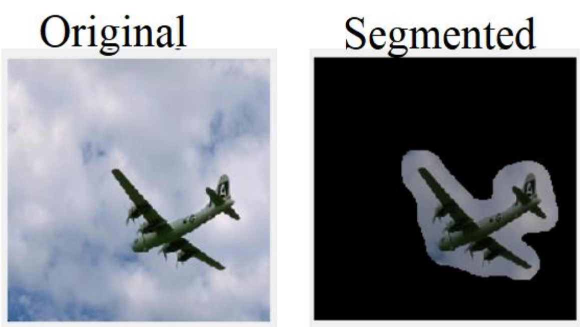

Figure 7. (b). Segmentation results for the Berkeley dataset

These visual results also indicate an improvement in the overall image segmentation performance, as only the regions of interest are extracted from the original image.

5. Conclusion and future scope

A large number of automatic image segmentation algorithms are application specific. This limits the applicability of these algorithms to real life datasets. The underlying algorithm removes this limitation with the help of a novel multi-domain image segmentation technique. The proposed technique improves the average PSNR by almost 10% when compared with existing state-of-the-art techniques. This also improves the PRI values, and reduces the overall MMSE when compared on Weizmann and Berkeley databases. Moreover, the proposed architecture uses a multi-class SVM with mode-based selection to select the best segmenter for the given input features. Accuracy of the proposed classifier further can be tested on other datasets. Also, more algorithms can be added to the ensemble learning mechanism for better segmentation performance. Moreover, the proposed classifier can be further improved using deep-learning techniques like convolutional neural networks (CNNs) and Q-learning can be used for better algorithmic optimization.

References

1. Bezdek, James & Hall, L & Clark, Matthew &Goldgof, Dmitry & Clarke, Laurence. (1997). Medical image analysis with fuzzy models. Statistical methods in medical research. 6. 191-214. 10.1191/096228097677057357.
2. ÖLMEZ, E., AKDOĞAN, V., KORKMAZ, M. et al. Automatic Segmentation of Meniscus in Multispectral MRI Using Regions with Convolutional Neural Network (R-CNN). J Digit Imaging 33, 916–929 (2020). https://doi.org/10.1007/s10278-020-00329-x
3. Mújica-Vargas, D., Kinani, J.M.V. & Rubio, J.d.Color-Based Image Segmentation by Means of a Robust Intuitionistic Fuzzy C-means Algorithm. Int. J. Fuzzy Syst. 22, 901–916 (2020). https://doi.org/10.1007/s40815-020-00824-x
4. Zeineldin, R.A., Karar, M.E., Coburger, J. et al. DeepSeg: deep neural network framework for automatic brain tumor segmentation using magnetic resonance FLAIR images. Int J CARS 15, 909–920 (2020). https://doi.org/10.1007/s11548-020-02186-z
5. Srinivas, B., Sasibhushana Rao, G. Segmentation of Multi-Modal MRI Brain Tumor Sub-Regions Using Deep Learning. J. Electr. Eng. Technol. 15, 1899–1909 (2020). https://doi.org/10.1007/s42835-020-00448-z
6. Flannery SW, Kiapour AM, Edgar DJ, Murray MM, Fleming BC. Automated magnetic resonance image segmentation of the anterior cruciate ligament. J Orthop Res. 2020 Nov 26. doi: 10.1002/jor.24926. Epub ahead of print. PMID: 33241856.
7. Machine Learning Techniques for Biomedical Image Segmentation: An Overview of Technical Aspects and Introduction to State-of-Art Applications, https://arxiv.org/abs/1911.02521
8. Liu C, Zhao R, Pang M. A fully automatic segmentation algorithm for CT lung images based on random forest. Med Phys. 2020 Feb;47(2):518-529. doi: 10.1002/mp.13939. Epub 2019 Dec 29. PMID: 31788807.
9. T. Lei, P. Liu, X. Jia, X. Zhang, H. Meng and A. K. Nandi, "Automatic Fuzzy Clustering Framework for Image Segmentation, in IEEE Transactions on Fuzzy Systems, vol. 28, no. 9, pp. 2078-2092, Sept. 2020, doi: 10.1109/TFUZZ.2019.2930030.

10. Unsupervised Learning of Image Segmentation Based on Differentiable Feature Clustering, https://arxiv.org/abs/2007.09990
11. Nikbakhsh, N., Baleghi, Y. &Agahi, H. A novel approach for unsupervised image segmentation fusion of plant leaves based on G-mutual information. Machine Vision and Applications 32, 5 (2021). https://doi.org/10.1007/s00138-020-01130-0
12. Unsupervised Image Segmentation using Mutual Mean-Teaching, https://arxiv.org/abs/2012.08922
13. L. Zhou and W. Wei, "DIC: Deep Image Clustering for Unsupervised Image Segmentation," in IEEE Access, vol. 8, pp. 34481-34491, 2020, doi: 10.1109/ACCESS.2020.2974496.
14. Khatibi, T, Rezaei, N, AtaeiFashtami, L, Totonchi, M. Proposing a novel unsupervised stack ensemble of deep and conventional image segmentation (SEDCIS) method for localizing vitiligo lesions in skin images. Skin Res Technol. 2020; 00: 1– 12. https://doi.org/10.1111/srt.12920
15. Ganjee, R., Ebrahimi Moghaddam, M. and Nourinia, R. (2020), An unsupervised hierarchical approach for automatic intra retinal cyst segmentation in spectral domain optical coherence tomography images. Med. Phys., 47: 4872-4884. https://doi.org/10.1002/mp.14361
16. Huawu Deng and D. A. Clausi, Unsupervised image segmentation using a simple MRF model with a new implementation scheme, Proceedings of the 17th International Conference on Pattern Recognition, 2004. ICPR 2004., Cambridge, 2004, pp. 691-694 Vol.2, doi: 10.1109/ICPR.2004.1334353.
17. Vigneshwaran, S, Govindaraj, V, Murugan, PR, Zhang, Y, Arun Prasath, T. Unsupervised learning-based clustering approach for smart identification of pathologies and segmentation of tissues in brain magnetic resonance imaging. Int J Imaging Syst Technol. 2019; 29: 439–456. https://doi.org/10.1002/ima.22321
18. Image Segmentation Algorithm Based on Superpixel Clustering, https://www.researchgate.net/publication/326486225_Image_Segmentation_Algorithm_Based_on_Superpixel_Clustering
19. Lefèvre S. (2010) A New Approach for Unsupervised Classification in Image Segmentation. In: Guillet F., Ritschard G., Zighed D.A., Briand H. (eds) Advances in Knowledge Discovery and Management. Studies in Computational Intelligence, vol 292. Springer, Berlin, Heidelberg. https://doi.org/10.1007/978-3-642-00580-0_7
20. Croitoru, I., Bogolin, SV. &Leordeanu, M. Unsupervised Learning of Foreground Object Segmentation. Int J Comput Vis 127, 1279–1302 (2019). https://doi.org/10.1007/s11263-019-01183-3
21. Mumford-Shah Loss Functional for Image Segmentation with Deep Learning, https://arxiv.org/abs/1904.02872
22. M. Pereyra and S. McLaughlin, Fast Unsupervised Bayesian Image Segmentation With Adaptive Spatial Regularisation, in IEEE Transactions on Image Processing, vol. 26, no. 6, pp. 2577-2587, June 2017, doi: 10.1109/TIP.2017.2675165.
23. M. Gadermayr, L. Gupta, V. Appel, P. Boor, B. M. Klinkhammer and D. Merhof, "Generative Adversarial Networks for Facilitating Stain-Independent Supervised and Unsupervised Segmentation: A Study on Kidney Histology," in IEEE Transactions on Medical Imaging, vol. 38, no. 10, pp. 2293-2302, Oct. 2019, doi: 10.1109/TMI.2019.2899364.

24. Deep-learning-based image segmentation integrated with optical microscopy for automatically searching for two-dimensional materials, https://www.nature.com/articles/s41699-020-0137-z
25. Alqazzaz, S., Sun, X., Yang, X. et al. Automated brain tumor segmentation on multi-modal MR image using SegNet. Comp. Visual Media 5, 209–219 (2019). https://doi.org/10.1007/s41095-019-0139-y
26. Hussain Hassan, N.M. Highly-efficient technique for automatic segmentation of X-ray bone images based on fuzzy logic and an edge detection technique. MultidimSyst Sign Process 31, 591–617 (2020). https://doi.org/10.1007/s11045-019-00677-0
27. Zhang, J., Zhou, Y., Xia, K. et al. A novel automatic image segmentation method for Chinese literati paintings using multi-view fuzzy clustering technology. Multimedia Systems 26, 37–51 (2020). https://doi.org/10.1007/s00530-019-00627-7
28. Robinson, R., Valindria, V.V., Bai, W. et al. Automated quality control in image segmentation: application to the UK Biobank cardiovascular magnetic resonance imaging study. J Cardiovasc MagnReson 21, 18 (2019). https://doi.org/10.1186/s12968-019-0523-x
29. Fully-Automatic Raw G-Band Chromosome Image Segmentation,https://www.researchgate.net/publication/340403050_Fully-Automatic_Raw_G-Band_Chromosome_Image_Segmentation
30. Sousa, A.M., Martins, S.B., Falcão, A.X., Reis, F., Bagatin, E. and Irion, K. (2019), ALTIS: A fast and automatic lung and trachea CT image segmentation method. Med. Phys., 46: 4970-4982. https://doi.org/10.1002/mp.13773.